recycling

MDPI

Article

Comprehensive Assessment and Long-Term Monitoring of High-Red-Brick-Content Recycled Aggregates from Rural Construction and Demolition Waste: A Study on Inorganic Composite Material Performance

Pengfei Li [1,2], Jie Ji [3,4,*], Daiyue Wang [1,2,*], Chuan Qiu [5], Ran Zhang [3,4] and Yanling Li [6]

[1] Beijing Xinqiao Technology Development Co., Ltd., Beijing 100088, China; lipengfei3060@163.com
[2] Research and Development Center of Transport Industry of Automated Construction Technology, Beijing 100088, China
[3] School of Civil and Transportation Engineering, Beijing University of Civil Engineering and Architecture, Beijing 100044, China; zhangran@bucea.edu.cn
[4] Engineering Technology Innovation Center of Construction and Demolition Waste Recycling, Ministry of Housing and Urban-Rural Development, Beijing University of Civil Engineering and Architecture, Beijing 100044, China
[5] Beijing Gonglian Jieda Highway Maintenance Engineering Co., Ltd., Beijing 100160, China; qc5530@163.com
[6] BCEG Resources Recycling Co., Ltd., Beijing 100083, China; liyanling@bcerr.cn
* Correspondence: jijie@bucea.edu.cn (J.J.); wang.yx@rioh.cn (D.W.)

Abstract

The durability characteristics of inorganic mixtures incorporating recycled aggregates from rural residential construction and demolition waste with high red brick content remain inadequately elucidated. To illuminate their long-term serviceability, two types of recycled aggregate inorganic mixtures (RAIMs) were formulated and implemented in a test road section, with their mechanical properties and fatigue resistance systematically monitored and assessed. Comparative analysis indicated that RAIMs exhibit comparable resistance to permanent deformation and analogous fracture failure mechanisms to natural aggregate inorganic mixtures (NAIMs), yet their elastic deformation recovery capability is compromised. Specifically, RAIMs attained parity with NAIMs in terms of unconfined compressive strength, indirect tensile strength, flexural tensile strength, and static compressive resilient modulus. However, their dynamic compressive resilient modulus, indirect tensile resilient modulus, and flexural tensile resilient modulus were lower than those of NAIMs by over 30%. Furthermore, probabilistic fatigue prediction models for RAIMs were established, facilitating reliable estimation of the service life of RAIMs under various stress intensity levels. This study holds considerable significance for dispelling the inherent perception of RAIMs' inferior service performance and augmenting the theoretical foundation for their resourceful utilization in road engineering.

Keywords: construction and demolition waste; recycled aggregate; high red brick content; inorganic mixture; service performance; long-term monitoring

Academic Editors: José Neves and Ana Cristina Freire

Received: 10 December 2025
Revised: 29 January 2026
Accepted: 2 February 2026
Published: 5 March 2026

1. Introduction

As the largest and most concentrated solid waste in China, the resource utilization of construction and demolition waste (CDW) is crucial for overcoming resource and environmental constraints. According to incomplete statistics, the existing stock of CDW in China has exceeded 20 billion tons, with an annual growth rate of 3.5 billion tons. However, its

total utilization rate is only approximately 40%, significantly lower than the 90% in EU countries and 97% in Japan [1,2]. The accumulation and storage of massive CDW not only wastes resources but also severely damages the ecological environment.

China is a major transportation country, requiring the construction and maintenance of nearly 400,000 km of roads annually, which consumes approximately 5 billion tons of natural sand and gravel. CDW can be processed into recycled aggregates of various particle sizes through specific technologies to replace natural sand and gravel in road engineering [3]. This approach not only absorbs large quantities of CDW with diverse types and qualities and reduces construction costs, but also mitigates environmental damage caused by natural aggregate mining. In recent years, numerous scholars have conducted extensive research on this topic. For instance, studies by Leite et al. [4] and Riviera et al. [5] demonstrated that the mechanical properties of RAIMs containing red bricks and concrete can meet the technical requirements for road bases and subbases, which was further confirmed by Pasetto and Baldo [6] and Xiao et al. [7]. However, Xiao et al. [7] also noted that the mechanical properties of RAIMs first increase and then decrease with the increase in recycled aggregate content, recommending a dosage range of 30–60%. Zeng et al. [8] similarly proposed controlling the recycled aggregate content between 40 and 60% to achieve optimal mechanical properties. Additionally, Zhang et al. [9] and Disfani et al. [10] found that the presence of red bricks affects the strength and water stability of RAIMs, suggesting that the red brick content should not exceed 50% of the total mass of red bricks and concrete. Xuan et al. [11] also recommended reducing red brick content in RAIMs to improve the mixture's mechanical performance.

While recycled aggregates from CDW have shown good applicability in road bases, most studies only advocate partial replacement of natural aggregates with recycled aggregates (dosage $\leq$ 60%). There are few applications of recycled aggregates with full-size particle combinations (100% CDW-derived recycled coarse and fine aggregates mixed in different mass proportions). This is attributed to the physical and chemical properties of source CDW, natural weathering, and CDW processing/crushing factors, which result in recycled aggregates having poorer road performance indicators (e.g., water absorption, crushing value, Los Angeles abrasion value) compared to natural aggregates. Moreover, waste red bricks exhibit higher crushing values, greater water absorption, and weaker adhesion to binders than waste concrete [12], leading to the recommendation that red brick content should not exceed 50% of the total mass of red bricks and concrete. However, current demolition projects in most regions primarily target rural residences, where red bricks are the main structural material, accounting for an average of over 60%—approximately twice the proportion of concrete. Given the immaturity of existing concrete-red brick separation technology, it is difficult to control or reduce red brick content through pre-treatment during the resource utilization of rural residential CDW. Furthermore, most existing research focuses on laboratory tests, with a lack of data supporting the long-term service effects of CDW-derived recycled aggregates—particularly limited tracking evaluations of performance after application in actual projects. The absence of clear durability indicators has led to an awkward situation where recycled aggregates are technically feasible but rarely adopted in practical projects due to concerns about performance. This social phenomenon has restricted the application of CDW in road engineering, hindering road construction from serving as the largest-scale technical channel for CDW consumption.

To clarify the applicability of full-size particle combination RAIMs in road bases and their long-term service effects, this study focuses on rural residential CDW with high red brick content (approximately 70 wt%). First, the classification and composition of CDW were statistically analyzed. Then, two types of full-size particle combination RAIMs (cement-treated and lime-fly ash-treated) were designed and optimized through laboratory

tests. Finally, these RAIMs were applied to the base of a heavy-load secondary road, and their mechanical properties at the initial service stage, as well as mechanical and fatigue properties after 3 years of service, were monitored and evaluated. This study clarifies the specific service performance indicators of high-red-brick-content RAIMs, which is of great significance for breaking the inherent perception of their poor service performance and enriching the theoretical basis for their resource utilization in road engineering.

2. Test Road Application

2.1. Test Road Design

To track and evaluate the service performance of RAIMs, a test road was designed and constructed within the Sunhe Township Construction Waste Resource Disposal Center (Chaoyang District, Beijing). The road was designed as a secondary road under heavy traffic conditions, with a double-width asphalt concrete pavement (total length = 140.0 m, width = 6.0 m, thickness = 0.6 m). Two structural configurations were adopted: CRAMs and L&FRAMs were used as the bases for the east and west road sections, respectively. The specific pavement structure combination is shown in Figure 1.

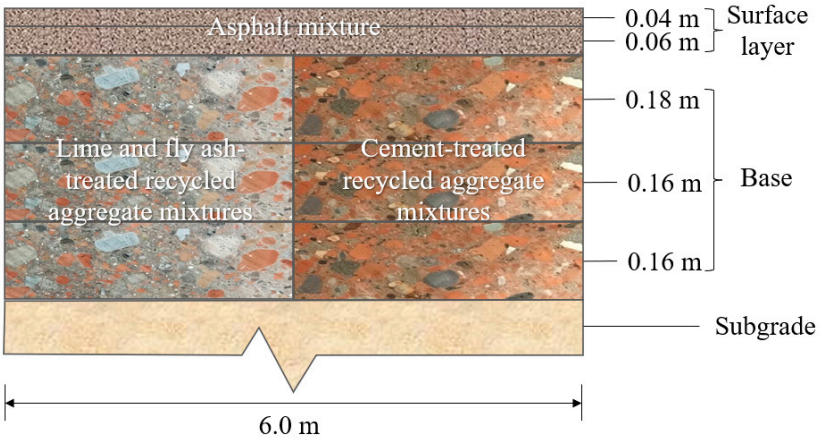

Figure 1. Schematic of test road pavement structure.

2.2. Service Conditions

The test road was completed in October 2019, officially put into use in January 2020, and monitored until December 2022. The service conditions (load and freeze–thaw cycles) are critical for evaluating post-service performance, as detailed below.

2.2.1. Load Condition

The primary service vehicles were CDW-carrying inbound and outbound trucks, with the following characteristics:

(1) Total vehicle trips: 86,634 (average of ~96 trips per day, calculated based on 10 months of annual operation).
(2) Vehicle load: Average load = 75 tons, maximum load = 160 tons. Vehicles with a net weight below 20 tons were six-wheel dump trucks; those between 20 and 50 tons were ten-wheel dump trucks; and those above 70 tons were semi-trailers.

2.2.2. Freeze–Thaw Conditions

Meteorological data from Beijing Station (2020–2022) was obtained from the China Meteorological Data Network. The temperature at a pavement depth of 0.28 m (corresponding to the bottom of the upper base layer of the test road) was calculated using the Park pavement temperature prediction model (Equation (1)) [13], which has good applicability to

various climatic and geographical conditions. Freeze–thaw cycles were defined following Chen [14]: a daily maximum temperature (T_{pmax}) > 0 °C and daily minimum temperature (T_{pmin}) < 0 °C indicate a freeze–thaw cycle at that pavement depth.

$$T_d = T_s + (0.00196d^3 - 0.0432d^2 - 0.3451d) \cdot \sin(-6.3252t + 5.0967) \quad (1)$$

where T_d is the temperature at depth d (°C); T_s is the temperature at the statistical time (°C); and t is a time parameter, for example, when the statistical time is 23:30, t = 23.5/24 = 0.9792.

The temperature variation in the test road base during service is shown in Figure 2. A total of 84 intersections between the 0 °C line and the temperature curve met the above freeze–thaw cycle criteria, indicating that 42 freeze–thaw cycles occurred during the service period.

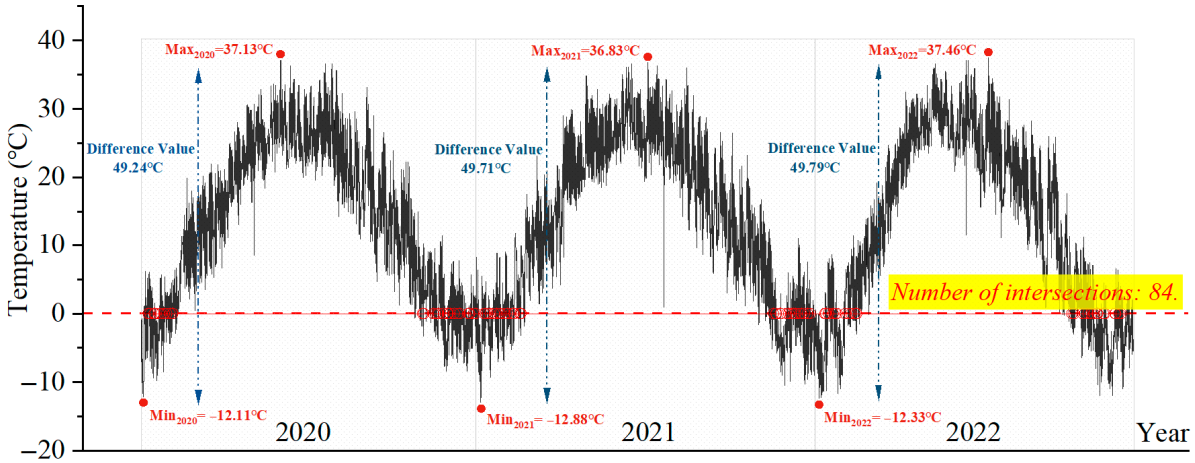

Figure 2. Temperature variations in the test road base during service.

3. Results and Discussions

3.1. Mechanical Properties of RAIMs at Initial Service Stage

After paving the test road base, compaction degree, cement content, lime content, and deflection were tested. The results (Table 1) show that all relevant construction control indicators comply with the Chinese industrial standard "Technical Guidelines for Construction of Highway Roadbases" (JTG/T F20-2015) [15]. Red bricks were visible in the core samples, with no crushing damage despite their high crushing value (Figure 3), indicating good integrity of the RAIM core samples.

Table 1. Construction control indicators of the test road base.

Parameters		Compaction Degree, %	Cement Content, %	Lime Content, %	Deflection Value, 0.01 mm
Test result	CRAMs	99.8	5.0	–	24.6
	L&FRAMs	99.2	–	5.0	27.2
Specification	CRAMs	≥98	4.0–5.0	4.0–5.0	≤29.5
	L&FRAMs				≤30.3

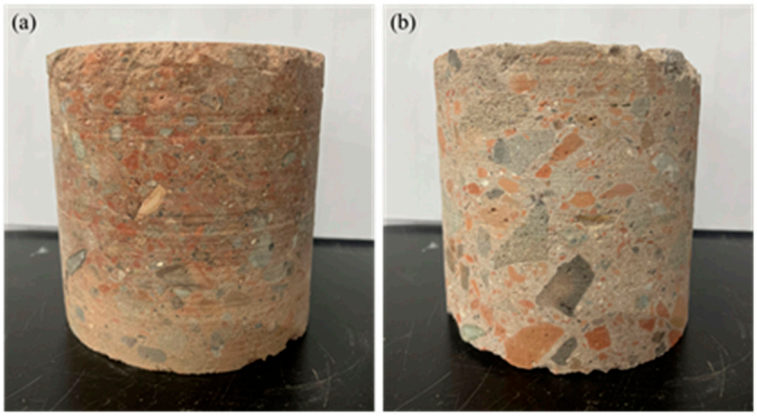

Figure 3. Integrity of RAIM core samples. (**a**) CRAMs; (**b**) L&FRAMs.

3.1.1. Unconfined Compressive Strength

The UCS of RAIMs at 7 d and 28 d ages was tested, with results presented in Table 2. Both CRAMs and L&FRAMs meet the specification and design requirements for secondary and lower-grade road bases under heavy traffic conditions. Notably, the UCS of L&FRAMs also meets the requirements for extremely heavy/extra-heavy traffic conditions and higher-grade roads. This may be attributed to the microporous structure of recycled aggregates, which facilitates the adsorption of cementitious binders, stabilizes the hydration and self-curing environment of binders, and promotes the formation of a strong interfacial system [16,17].

Table 2. UCS of RAIMs.

Parameters	Test Result		Specification		Test Method
	CRAMs	L&FRAMs	CRAMs	L&FRAMs	
7 d age, MPa	3.7	1.8	3.0–5.0/≥3.4	≥0.8/≥1.0	T0805
28 d age, MPa	4.9	3.2	−/≥3.4	−/≥2.7	

Note: Values before "/" refer to JTG/T F20-2015 requirements; values after "/" refer to design requirements.

As shown in Figure 4, the UCS of RAIMs is slightly lower than that of NAIMs (difference in only a few tenths of a MPa). This is because recycled aggregates have more surface and internal microcracks, and poorer road performance indicators (e.g., water absorption, crushing value) compared to natural aggregates, due to the physical and chemical properties of source CDW, natural weathering, and processing factors [2].

Additionally, for both RAIMs and NAIMs, the UCS of cement-treated mixtures is higher than that of lime-fly ash-treated mixtures at the same age. This is because the strength of cement hydration products is higher than that of lime-fly ash pozzolanic reaction products. The UCS of both mixtures increases with age: the 28 d UCS of cement-treated mixtures is approximately 1.3 times the 7 d UCS, while the 28 d UCS of lime-fly ash-treated mixtures is approximately 1.8 times the 7 d UCS (showing greater growth). This is due to the faster hydration rate of cement (reaching ~70% of design strength at 7 d), whereas lime-fly ash strength grows more slowly in the first 7 d [18].

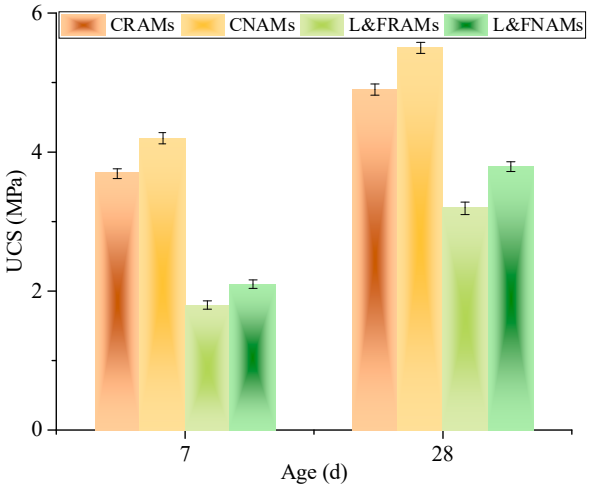

Figure 4. Comparison of UCS between RAIMs and NAIMs.

3.1.2. Compressive Resilient Modulus

Figure 5 shows the static compressive resilient modulus (SCRM) of NAIMs and RAIMs tested via the top surface method. The SCRM of NAIMs is slightly higher than that of RAIMs (difference < 3%), and both meet or slightly exceed the design reference values for CRM of cement-treated crushed stone (cement content: 4–6%) and lime-fly ash-treated crushed stone (lime content: 8%, fly ash content: 17%) specified in "Code for Pavement Design of Urban Road" (CJJ 169-2011) (1300–1700 MPa and 1100–1500 MPa, respectively) [19]. This indicates that RAIMs have sufficient stiffness. Similar to UCS, the CRM of cement-treated mixtures is higher than that of lime-fly ash-treated mixtures due to the higher strength of cement hydration products.

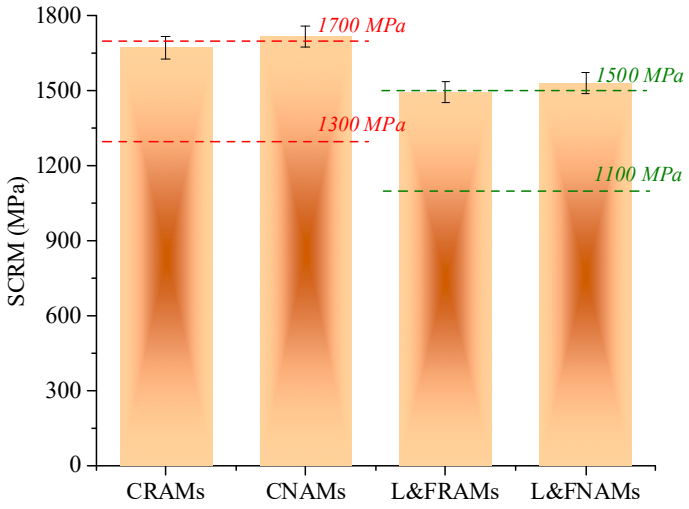

Figure 5. Comparison of SCRM between RAIMs and NAIMs.

3.1.3. Frost Resistance

Under the influence of precipitation, road bases may remain saturated for long periods. Free water within the base can freeze in winter, causing structural damage and partial or total loss of strength [20,21]. Therefore, the Chinese industrial standard "Specification for Design of Highway Asphalt Pavement" (JTG D50-2017) [22] requires frost resistance testing of inorganic mixtures in severe and moderate freezing regions. The test road is located in a moderate freezing region (a subcategory of seasonal frozen soil regions with the freezing index F ranging from 800 to 2000 °C·d), and CDW-derived recycled aggregates have high water absorption—making full-size particle combination RAIMs more prone to retaining

free water and experiencing frost heave at low temperatures. Thus, the frost resistance of RAIMs was evaluated using the residual compressive strength ratio (ratio of compressive strength before and after freeze–thaw) and mass change rate (Table 3, Figure 6).

Table 3. Frost resistance of RAIMs.

Parameters		5 Freeze–Thaw Cycles		10 Freeze–Thaw Cycles	
		Residual Compressive Strength Ratio, %	Mass Change Rate, %	Residual Compressive Strength Ratio, %	Mass Change Rate, %
Test result	CRAMs	93.3	0.2	87.1	0.8
	L&FRAMs	87.8	0.7	82.2	1.5
Specification	CRAMs		–		
	L&FRAMs	≥65	<5.0	≥65	<5.0

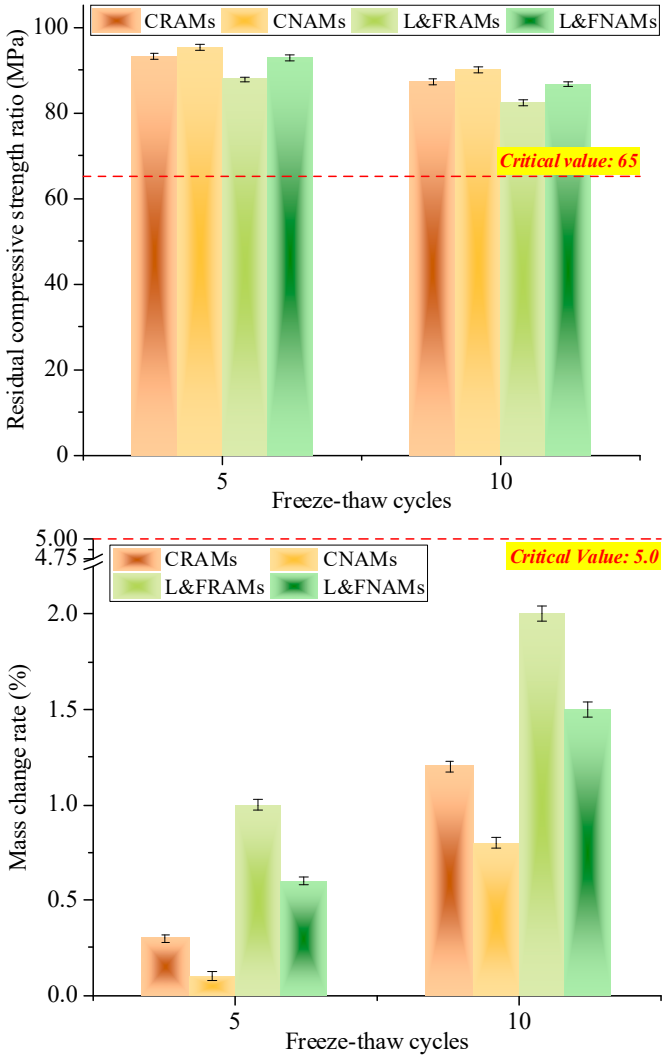

Figure 6. Comparison of frost resistance between RAIMs and NAIMs.

The frost resistance of mixtures is mainly influenced by porosity and aggregate water absorption. Despite the high water absorption of CDW-derived recycled aggregates, CRAMs and L&FRAMs exhibited minimal mass loss: CRAM samples showed no particle detachment or edge defects after freeze–thaw, while L&FRAM samples had slight local particle detachment but no loosening. Although the frost resistance of RAIMs is slightly lower than that of NAIMs, their residual compressive strength ratio and mass change rate far exceed the technical requirements for moderate freezing regions and also meet those for

severe freezing regions (residual compressive strength ratio ≥ 70%). This is attributed to the dense gradation of the mixtures (low void ratio) and the filling of recycled aggregate surface pores by cementitious products from the hydration of cement, lime, and fly ash—blocking internal–external connectivity and inhibiting water penetration [23]. Additionally, cement-treated mixtures have better frost resistance than lime-fly ash-treated mixtures due to the stronger hydration capacity of cement and superior overall mixture performance.

3.2. Mechanical and Fatigue Properties of RAIMs After 3 Years of Service

3.2.1. Disease and Deflection Conditions

To intuitively assess the structural integrity and stability of the test road base after 3 years of service, disease investigations and statistical analyses were conducted. The results show only four transverse cracks in the base (Table 4), which correspond to surface layer cracks (Figure 7). This indicates good structural integrity of the RAIM base, with no severe damage—fully meeting the requirements of heavy traffic conditions. Core samples taken at the transverse cracks revealed that the cracks did not penetrate the upper base layer, suggesting top-down crack initiation—likely caused by continuous heavy traffic loads during service.

Table 4. Statistics of typical road base diseases.

Serial Number	Position		Length, m	Disease Type
1	K0 + 074	Across the left and right lanes	6.0	Transverse crack
2	K0 + 088	Right lane	3.0	
3	K0 + 099	Across the left and right lanes	6.0	
4	K0 + 113		6.0	

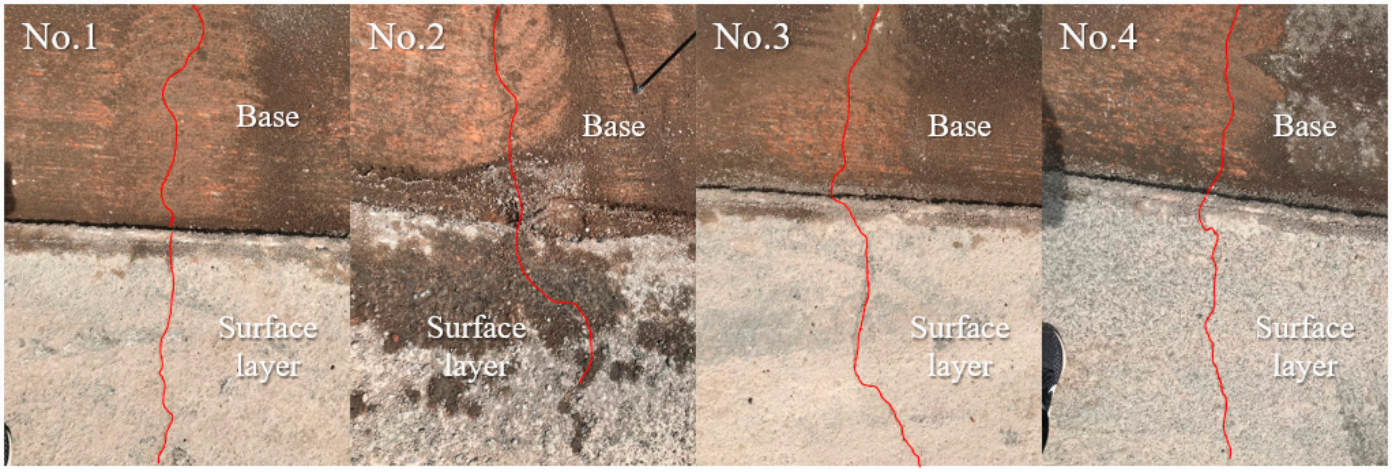

Figure 7. Schematic of typical road base diseases.

Deflection tests were conducted and compared with initial service values (Figure 8). The deflection values of the test road base decreased significantly after 3 years: 31.3% for the CRAM base and 17.3% for the L&FRAM base. This is because continuous vehicle loads promoted further interlocking and densification of the mixtures, enhancing the strength and stability of the structural layer [8].

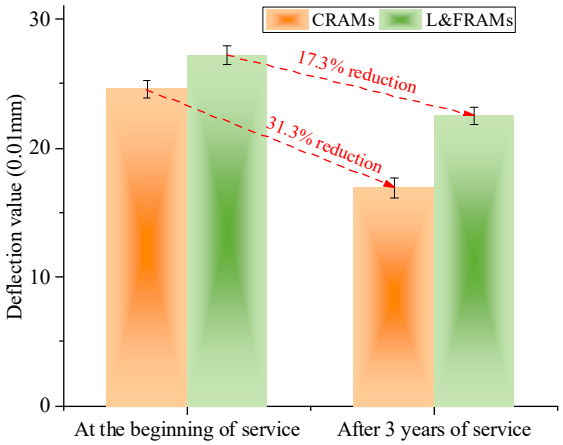

Figure 8. Deflection values of RAIMs before and after 3 years of service.

3.2.2. Mechanical Properties

Strength

The UCS, ITS, and FTS of RAIMs after 3 years of service are compared with those of NAIMs with similar service time and mixture composition in Figures 9–11 [24–27].

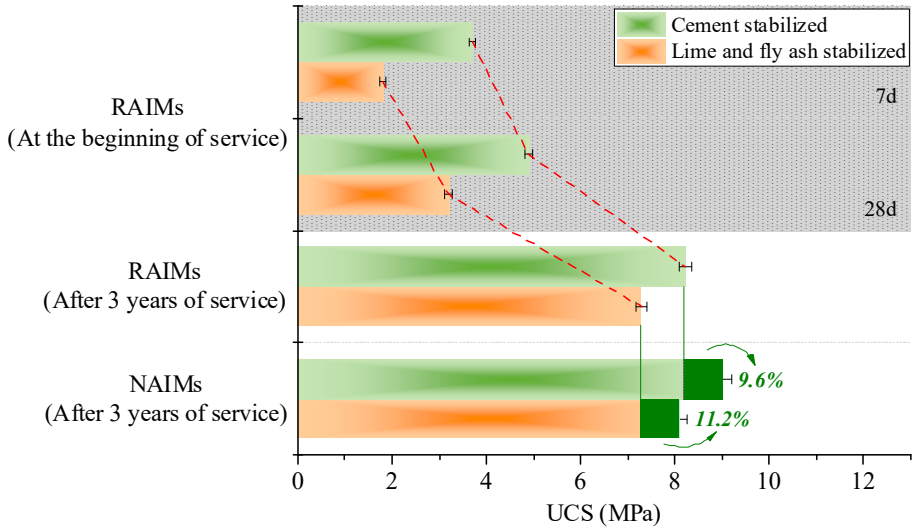

Figure 9. Comparison of UCS between RAIMs and NAIMs before and after service.

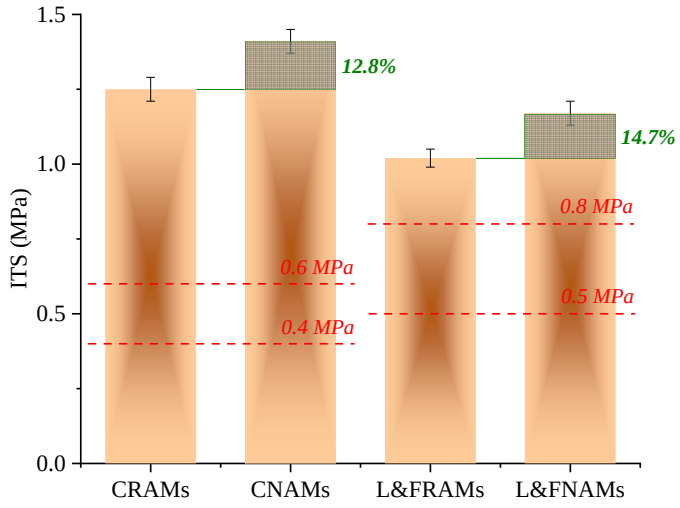

Figure 10. Comparison of ITS between RAIMs and NAIMs after service.

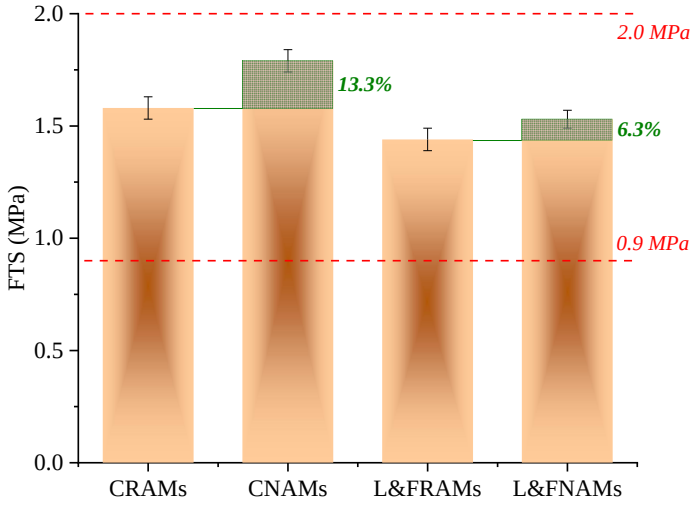

Figure 11. Comparison of FTS between RAIMs and NAIMs after service.

Overall, NAIMs still exhibit better resistance to permanent deformation and fracture than RAIMs after 3 years of service, due to the performance advantages of natural aggregates. However, the differences in UCS, ITS, and FTS between the two are insignificant (≤15%). Moreover, due to continuous traffic compaction and cementitious binder hydration, the UCS of RAIMs is significantly higher than that at initial service. The ITS of RAIMs exceeds the design reference values for cement-treated crushed stone (cement content: 4–6%) and lime-fly ash-treated crushed stone (lime content: 8%, fly ash content: 17%) specified in CJJ 169-2011 [19] (0.4–0.6 MPa and 0.5–0.8 MPa, respectively). Their FTS also falls within the range of 0.9–2.0 MPa specified in JTG D50-2017 [22] for cement-treated and lime-fly ash-treated materials. This indicates that despite the weakening effects of accumulated vehicle loads (86,634 trips) and freeze–thaw cycles (42 times), full-size particle combination RAIMs still maintain good mechanical strength.

Consistent with previous results, the UCS, ITS, and FTS of cement-treated mixtures are higher than those of lime-fly ash-treated mixtures, due to differences in the properties of cementitious binder hydration products.

Resilience Modulus

Figures 12–14 show the CRM, ITRM, and FTRM of RAIMs and NAIMs with similar service time and mixture composition [24,28,29]. The CRM of cement-treated mixtures is higher than that of lime-fly ash-treated mixtures, indicating better stiffness of cement-bound mixtures. The SCRM of RAIMs is comparable to that of NAIMs, but significant differences exist in dynamic compressive resilient modulus (DCRM), ITRM, and FTRM: the DCRM, ITRM, and FTRM of CNAMs are approximately 1.3, 1.3, and 1.4 times higher than those of CRAMs, while the DCRM of L&FNAMs is ~1.4 times higher than that of L&FRAMs. Although no direct reference values for the ITRM and FTRM of NAIMs were found, similar trends are inferred based on previous results. This indicates that RAIMs exhibit weaker resistance to elastic deformation than NAIMs and are more susceptible to cracking under repeated loading, in part attributed to the greater number of microcracks on the surface and inside recycled aggregates. These microcracks elevate the risk of aggregate fracture and binder detachment under cyclic loading. Nevertheless, RAIMs still meet service requirements. Relevant studies have also demonstrated that pores at different scales, crack connectivity, and interfacial damage contribute differently to the stiffness degradation of the mixture [30]. Accordingly, further in-depth mechanistic research on these aspects should be carried out in future work.

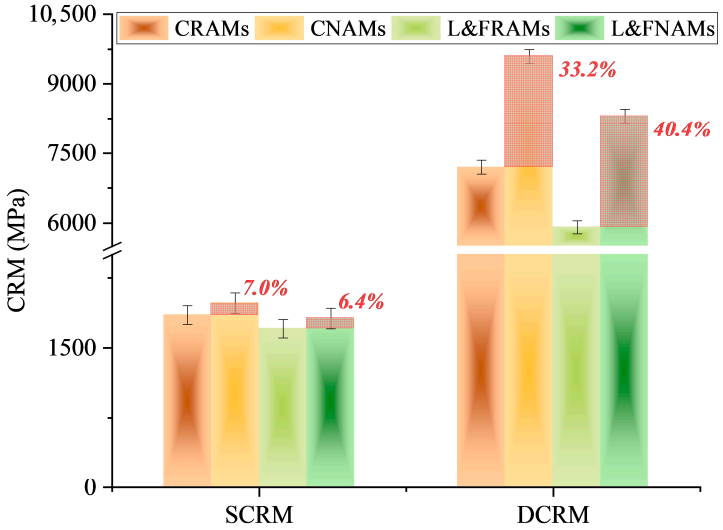

Figure 12. Comparison of CRM between RAIMs and NAIMs after service [24].

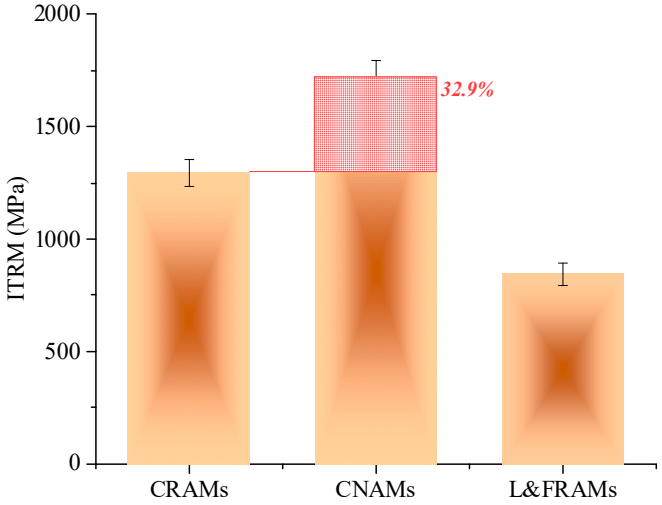

Figure 13. Comparison of ITRM between RAIMs and NAIMs after service [28].

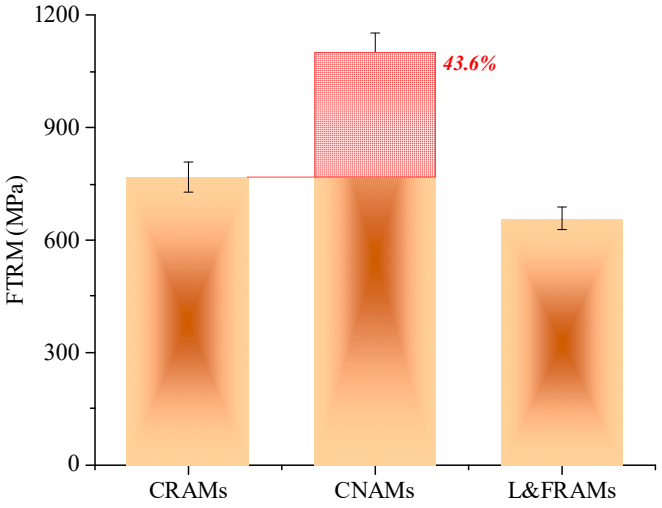

Figure 14. Comparison of FTRM between RAIMs and NAIMs after service [29].

3.2.3. Fatigue Properties

Fatigue property is a key indicator of pavement durability and reliability. The fatigue test results of RAIMs are shown in Figure 15, along with a comparison with NAIMs of similar service time and mixture composition [31].

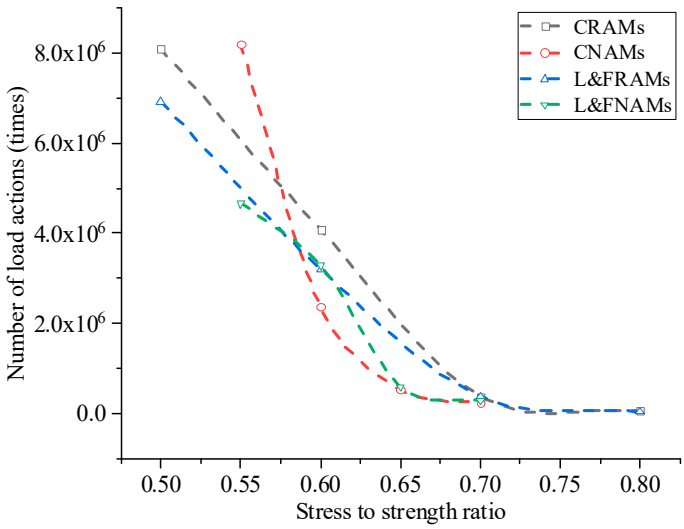

Figure 15. Fatigue properties of RAIMs and NAIMs.

As shown in Figure 15, the fatigue life of cement-treated mixtures is significantly higher than that of lime-fly ash-treated mixtures, but both maintain high levels of fatigue resistance. When the stress-to-strength ratio (σ/s) is small, the fatigue life difference between CRAMs and L&FRAMs is large (e.g., 1,176,400 more cycles for CRAMs when σ/s = 0.5). As σ/s increases, the gap narrows (e.g., only 4423 more cycles for CRAMs when σ/s = 0.7). NAIMs exhibit the same trend. This indicates that cement-treated mixtures have better fatigue resistance than lime-fly ash-treated mixtures, and that fatigue damage occurs rapidly for all mixtures when the applied load approaches the flexural tensile strength limit. Additionally, the fatigue life of RAIMs is slightly lower than that of NAIMs but remains comparable, demonstrating excellent durability and reliability of RAIMs.

To estimate the fatigue life of RAIMs under different load levels, regression analysis was performed on the fatigue test results using a single logarithmic equation, yielding fatigue equations with a 50% guarantee rate (Table 5). Compared with the NAIM fatigue equations (50% guarantee rate) reported by Wei [31], the lime-fly ash-treated mixture equations are nearly identical, while the cement-treated mixture equations differ slightly. However, the calculated fatigue life differences at the same stress level are minimal, confirming the reliable service performance of RAIMs. It should be noted that the fatigue equation established through regression analysis is an empirical, interval-dependent and single-scenario statistical model, which cannot be directly applied to the accurate prediction of pavement fatigue life under complex in-service environments.

Table 5. Fatigue equations of RAIMs and CAIMs.

Mixture Type	Fatigue Equation
CRAMs	$\lg N = 10.69 - 7.29\ (\sigma/s)$
CNAMs	$\lg N = 13.775 - 12.231\ (\sigma/s)$
L&FRAMs	$\lg N = 12.05 - 9.24\ (\sigma/s)$
L&FNAMs	$\lg N = 12.26 - 9.9563\ (\sigma/s)$

Note: N is the number of load cycles (times); σ is the flexural tensile stress (MPa); s is the flexural tensile strength (MPa).

4. Materials and Methods

4.1. Classification and Composition Analysis of CDW

To fully understand the classification and composition of rural residential CDW, samples were collected from Sunhe Township (Chaoyang District), Shahe Township (Changping

District), and Lehe Township (Pinggu District) in Beijing for systematic investigation and analysis. The building structures in these three demolition areas are representative of typical rural residential CDW: Sunhe Township and Shahe Township mainly consist of rural residences with a small number of factories and auxiliary buildings, while Lehe Township is entirely composed of rural residences. The statistical results are presented in Figure 16. Since waste concrete, red bricks, and mortar are the primary raw materials for preparing recycled aggregates, the proportions of these three components were also analyzed (Figure 17). It should be noted that CDW particles smaller than 100 mm are difficult to classify into specific types, with residual soil accounting for approximately 25–30% of the total CDW. Therefore, only the contents of waste concrete, red bricks, and mortar in particles larger than 100 mm were statistically analyzed.

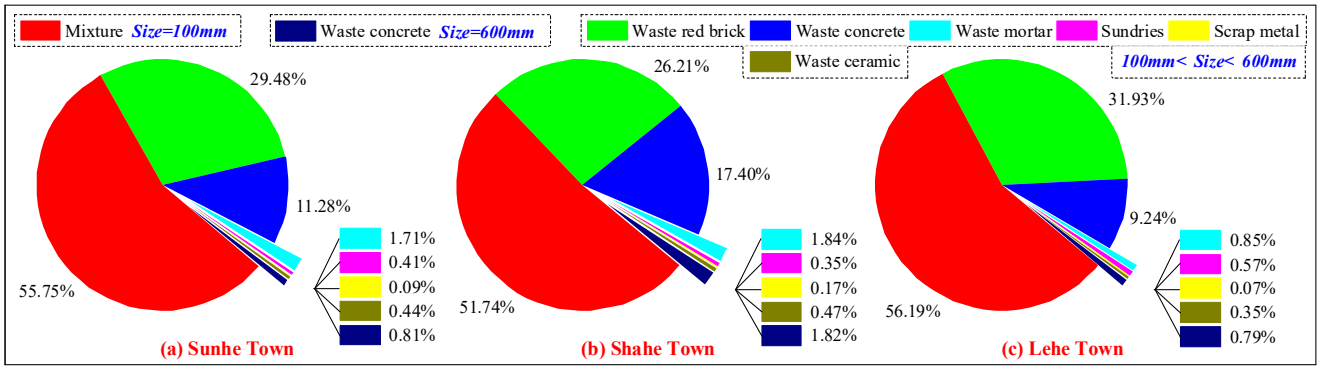

Figure 16. Classification and composition of CDW.

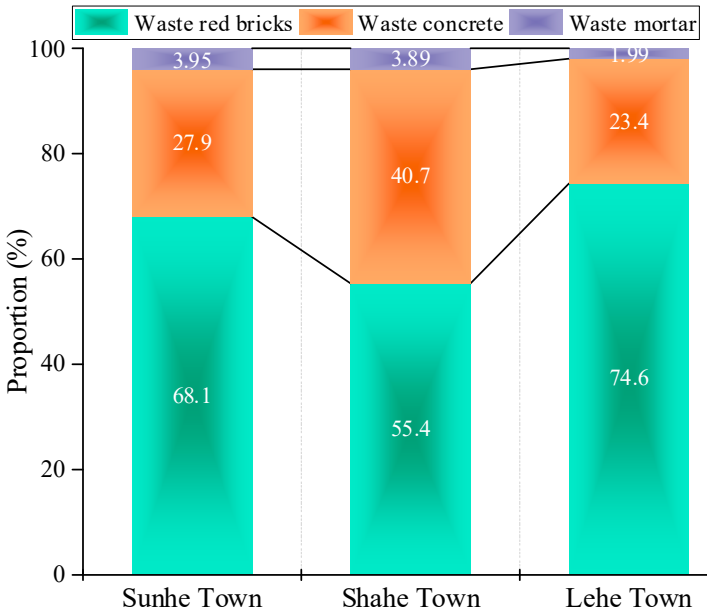

Figure 17. Proportion of waste red bricks, waste concrete, and waste mortar in recyclable CDW components.

The classification and composition of CDW in the three demolition areas showed good consistency. As shown in Figure 16, CDW can be categorized into three particle size ranges: <100 mm, 100–600 mm, and >600 mm, with over 98.86% of particles concentrated below 600 mm. CDW particles larger than 600 mm are mainly large, sortable waste concrete pieces, accounting for less than 2%. For a disposal line processing 700,000 tons of CDW annually, large waste concrete pieces amount to less than 15,000 tons. Sorting only large waste concrete pieces to prepare recycled aggregates is far from meeting market demand,

reflecting the limitations of CDW resource utilization when relying primarily on cement-based components.

In terms of composition, CDW can be divided into waste concrete, waste red bricks, waste mortar, waste ceramics, scrap metals, sundries, and mixtures of these substances. However, the amount of recyclable CDW is relatively small, accounting for less than 45% of the total. Among recyclable components, waste red bricks, waste concrete, and waste mortar account for approximately 55–75%, 23–40%, and 3–5%, respectively (Figure 17). This indicates that recyclable rural residential CDW is dominated by red bricks and concrete, with a high red brick content. Therefore, research on high-red-brick-content CDW is both reasonable and necessary.

4.2. Materials

4.2.1. Recycled Aggregate

The CDW used in this study was sourced from the demolition project in Sunhe Township, Chaoyang District, Beijing, and the recycled aggregates were produced by the Sunhe Township CDW Resource Disposal Center. The particle sizes of the recycled aggregates were 0–5 mm, 5–10 mm, 10–20 mm, and 20–31.5 mm (Figure 18).

Figure 18. CDW-derived recycled aggregates with different particle sizes.

The basic properties of the recycled aggregates were tested in accordance with the Chinese industrial standards "Test Methods for Aggregate for Highway Engineering" (JTG E42-2005) [32] and "Technical Specifications for Utilization of Construction Waste in Highway Engineering" (JTG/T 2321-2021) [33], with the results presented in Tables 6 and 7. It can be seen that the properties of the recycled aggregates meet the requirements for secondary and lower-grade road bases specified in JTG/T 2321-2021 [33].

Table 6. Properties of CDW-derived recycled coarse aggregates (particle size ≥ 4.75 mm).

Parameters	Apparent Relative Density	Water Absorption, %	Crushing Value, %	Needle Flake Particle Content, %	Dust Content Below 0.075 mm, %	Lightweight Miscellaneous Content, %	Recycled Concrete Particle Content, %
Test result	2.391	14.2	32.7	6.9	1.1	0.2	39.5
Specification	–	–	≤35	≤20	≤2.0	≤0.5	≥35
Test method	T0308	T0307	T0316	T0312	T0310	Appendix A of JTG/T 2321	

Table 7. Properties of CDW-derived recycled fine aggregates (particle size < 4.75 mm).

Parameters	Apparent Relative Density	Plasticity Index of Materials Below 0.075 mm	Sand Equivalent, %	Organic Matter Content, %	Sulfate Content, %	Mud Content, %
Test result	2.454	7.4	69.3	0.6	0.08	1.7
Specification	–	≤17	≥40	<2.0	≤0.25	≤3.0
Test method	T0328	T0118	T0334	T0336	T0341	T0335

4.2.2. Natural Aggregate

To compare the performance differences between RAIMs and NAIMs, inorganic mixtures were prepared using natural aggregates from Huairou District, Beijing. The basic properties of the natural aggregates were tested in accordance with JTG E42-2005 [32]. The test results for coarse aggregates are shown in Table 8; the fine aggregates were clean, dry, unweathered, and free of impurities, with particles below 0.075 mm accounting for 5.9%. The properties of the natural aggregates meet the requirements for secondary and lower-grade roads specified in JTG/T F20-2015 [15].

Table 8. Properties of natural coarse aggregates (particle size ≥ 4.75 mm).

Parameters	Apparent Relative Density	Water Absorption, %	Crushing Value, %	Needle Flake Particle Content, %	Dust Content Below 0.075 mm, %	Soft Stone Content, %
Test result	2.721	2.3	14.9	4.3	0.7	2.4
Specification	–	–	≤30	≤20	–	–
Test method	T0308	T0307	T0316	T0312	T0310	T0320

Compared with natural aggregates, the water absorption and crushing value of recycled aggregates are approximately 6.2 times and 2.2 times higher, respectively. Recycled aggregates, sourced from waste concrete, red bricks, and mortar with distinct material properties, account for this discrepancy: concrete contains high-strength, dense-structure aggregates (e.g., stones and pebbles), resulting in recycled aggregates with low crushing values and water absorption (accounting for less than 30%); red bricks are sintered products with low strength and porous internal structures, leading to recycled aggregates with high crushing values and water absorption (accounting for nearly 70%); mortar itself has low strength, and its crushed recycled aggregates also exhibit high crushing values and water absorption.

4.2.3. Cementitious Binder

Cement

Jidong 32.5-grade slag Portland cement was used, and its basic properties were tested in accordance with "Test Methods for Cement and Concrete for Highway Engineering" (JTG E30-2005) [34]. The results (Table 9) show that the cement meets the requirements for strength grade and setting time specified in JTG/T F20-2015 [15].

Table 9. Properties of cement.

Parameters	Cement Grade	Standard Consistency, %	Setting Time, min		Compressive Strength, MPa		Flexural Strength, MPa		Stability
			Initial Setting	Final Setting	3 d	28 d	3 d	28 d	
Test result	32.5	28.6	322	384	18.6	43.8	3.8	9.2	Qualified
Specification	32.5 or 42.5	–	>180	360–600			–		
Test method	–		T0505			T0506			T0505

Lime and Fly Ash

Magnesia quicklime (Grade III) was used as the lime, and silica-alumina fly ash was adopted. Both materials were tested in accordance with relevant methods in JTG E42-2005 [32], with the results presented in Tables 10 and 11. The properties of lime and fly ash comply with the requirements of JTG/T F20-2015 [15].

Table 10. Properties of lime.

Parameters	Content of Effective CaO and MgO, %	Undigested Residue Content, %	Content of MgO, %
Test result	66.98	14.27	5.26
Specification	≥65	≤20	>5
Test method	T0813	T0815	T0812

Table 11. Properties of fly ash.

Parameters	Total Content of SiO_2, Al_2O_3, and Fe_2O_3, %	Loss on Ignition, %	Specific Surface Area, cm^2/g	Passing Rate of 0.3 mm Sieve, %	Passing Rate of 0.075 mm Sieve, %	Moisture Content of Wet Fly Ash, %
Test result	90.57	7.5	4800	99.6	86.3	20.1
Specification	>70	≤20	>2500	≥90	≥70	≤35
Test method	T0816	T0817	T0820	T0818	T0818	T0801

4.3. Mixture Composition Design

4.3.1. Gradation Design

A skeleton-dense gradation was adopted. In accordance with JTG/T F20-2015 [15], the proportions of 0–5 mm, 5–10 mm, 10–20 mm, and 20–31.5 mm recycled aggregates in cement-treated and lime-fly ash-treated mixtures were determined as 35%, 30%, 25%, 10% and 25%, 30%, 30%, 15%, respectively. The designed gradations are shown in Figure 19. Cement-treated natural aggregate mixtures (CNAMs) and lime-fly ash-treated natural aggregate mixtures (L&FNAMs) were designed using the same gradation.

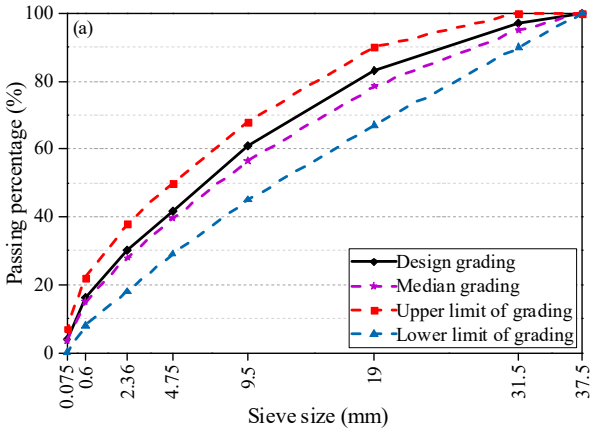

Figure 19. *Cont.*

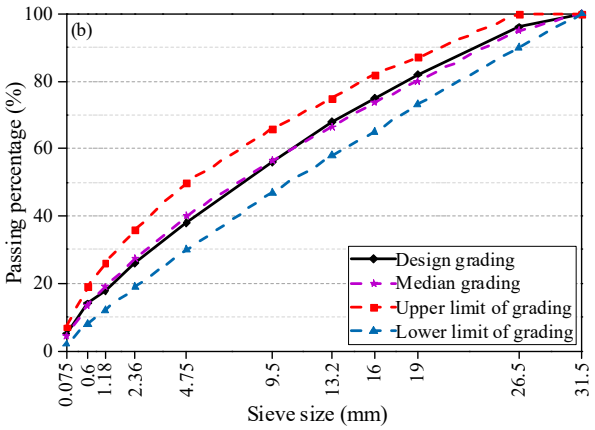

Figure 19. Designed gradations of RAIMs. (**a**) Cement-treated recycled aggregate mixtures (CRAMs); (**b**) lime and fly ash-treated recycled aggregate mixtures (L&FRAMs).

4.3.2. Mix Design

Based on preliminary laboratory tests and comprehensive performance evaluations of RAIMs, the optimal cement content for CRAMs was determined to be 5%, and the optimal lime and fly ash contents for L&FRAMs were 5% and 10%, respectively. These proportions were adopted as the construction ratios for the subsequent test road base, and the same ratios were used to prepare NAIMs. In accordance with "Test Methods of Materials Stabilized with Inorganic Binders for Highway Engineering" (JTG E51-2009) [35], the maximum dry density and optimal water content of the above inorganic mixtures were determined via heavy compaction tests (Table 12).

Table 12. Maximum dry density and optimal water content of inorganic mixtures.

Mixture Type	Cement Content, %	Lime Content, %	Fly Ash Content, %	Maximum Dry Density, g/cm^3	Optimal Water Content, %
CRAMs	5	–		1.768	14.1
L&FRAMs	–	5	10	1.742	13.8
CNAMs	5	–		2.345	5.8
L&FNAMs	–	5	10	2.321	5.9

4.4. Performance Evaluation Method

After paving the test road base, compaction degree, cement content, lime content, deflection, and core sample integrity were tested in accordance with JTG/T F20-2015 [15] to ensure construction quality. Meanwhile, key design indicators of RAIMs (e.g., unconfined compressive strength (UCS), compressive resilient modulus (CRM), and frost resistance) were tested to verify whether their basic mechanical properties at the initial service stage meet specification and design requirements. Additionally, to gain detailed insights into the service performance and long-term effects of RAIMs, disease investigations and deflection tests were conducted on the test road base after 3 years of service. Comprehensive mechanical and fatigue property tests were also performed on RAIMs, including UCS, indirect tensile strength (ITS), flexural tensile strength (FTS), CRM, indirect tensile resilient modulus (ITRM), flexural tensile resilient modulus (FTRM), and fatigue life. Note that all tests on RAIMs focused on the upper base layer.

4.4.1. Sample Preparation

Cylindrical samples (height = 150 mm, diameter = 150 mm) were used for UCS, ITS, CRM, ITRM, and frost resistance tests. NAIM samples were prepared via static compaction, while RAIM samples were obtained through core drilling. Core drilling at the initial service

stage was conducted after the RAIM base was paved and reached the specified curing age. For samples after 3 years of service, the asphalt pavement surface layer was first milled, and debris/dust on the upper base layer was cleaned (Figure 20) before core drilling. A total of 142 samples were prepared.

Figure 20. Schematic of core drilling and sampling process. (**a**) Pavement milling; (**b**) Core drilling and sampling.

Beam-shaped samples (length = 550 mm, width = 150 mm, height = 150 mm) were used for FTS, FTRM, and fatigue property tests, obtained through cutting and sampling (Figure 21). For the test road with 3 years of service, the pavement surface was also milled and cleaned prior to sampling. A total of 82 samples were prepared.

Figure 21. Schematic of the cutting and sampling process.

As specified in JTG E51-2009 [35], the obtained RAIM samples were refined (cutting, plastering, etc.) before performance testing (Figure 22).

Figure 22. Sample refinement. (**a**) Cylindrical samples. (**b**) Beam-shaped samples.

4.4.2. Test Methods

Tests for compaction degree, cement content, lime content, deflection, and core sample integrity followed the requirements of JTG/T F20-2015 [15]. For deflection testing after

3 years of service, pavement surface milling was required first. Other performance tests were conducted in accordance with JTG E51-2009 [35], and detailed procedures are not repeated herein.

5. Conclusions and Recommendations

(1) Rural residential CDW mainly consists of waste red bricks, waste concrete, waste mortar, and their mixtures. Among these, the components suitable for road engineering recycling are waste red bricks (55–75%), waste concrete (23–40%), and waste mortar (3–5%).

(2) At the initial service stage, the UCS, CRM, and frost resistance of RAIMs are slightly lower than those of NAIMs but all meet specification and design requirements, and the frost resistance of RAIMs far exceeds technical standards.

(3) After 3 years of service, the UCS, ITS, FTS, and SCRM of RAIMs are comparable to those of NAIMs, but their DCRM, ITRM, and FTRM are reduced by more than 30% compared to NAIMs. This indicates that RAIMs have equivalent resistance to permanent deformation and fracture to NAIMs but poorer elastic deformation resistance. Targeted physicochemical modification of recycled aggregates, coupled with dense-graded mix design and the incorporation of composite rubber powder into the cementitious system, effectively alleviates such elastic deformation under repeated loading.

(4) RAIMs exhibit fatigue life comparable to that of NAIMs. The fatigue equations for CRAMs ($\lg N = 10.69 - 7.29\ (\sigma/s)$) and L&FRAMs ($\lg N = 12.05 - 9.24\ (\sigma/s)$) were established, enabling the estimation of RAIM fatigue life under different load levels and providing a theoretical basis for evaluating their long-term service effects.

This study clarifies the engineering applicability of full-gradation RAIMs derived from high-red-brick-content CDW for road base layers, with a specific focus on their long-term service performance, thereby enriching the theoretical basis for their resource utilization in road engineering. However, the conclusions of this study are based on a limited range of application scenarios. Future research will investigate the service performance of RAIMs in higher-grade roads, different climatic conditions, and longer service periods to generalize the findings. Additionally, theoretical studies on the mechanisms underlying RAIM service performance changes should be conducted.

Author Contributions: Conceptualization, P.L. and J.J.; methodology, P.L., J.J. and D.W.; validation, C.Q.; formal analysis, R.Z.; investigation, P.L. and Y.L.; resources, C.Q. and Y.L.; data curation, R.Z.; writing—original draft preparation, P.L.; writing—review and editing, J.J. and D.W.; project administration, J.J.; funding acquisition, J.J. All authors have read and agreed to the published version of the manuscript.

Funding: This research was funded by the National Key R&D Program of China (2022YFC3803403), the National Natural Science Foundation of China (52078025), the Project of Construction and Support for High-level Innovative Teams of Beijing Municipal Institutions (BPHR20220109), and the Cultivation Project Funds for Beijing University of Civil Engineering and Architecture (X23036).

Data Availability Statement: The original contributions presented in this study are included in the article. Further inquiries can be directed to the corresponding authors.

Conflicts of Interest: Pengfei Li and Daiyue Wang work at Beijing Xinqiao Technology Development Co., Ltd. Chuan Qiu works at Beijing Gonglian Jieda Highway Maintenance Engineering Co., Ltd. Yanling Li works at BCEG Resources Recycling Co., Ltd. The remaining authors declare that the research was conducted in the absence of any commercial or financial relationships that could be construed as potential conflict of interest.

References

1. Peng, Z.; Lu, W.; Webster, C.J. Quantifying the embodied carbon saving potential of recycling construction and demolition waste in the Greater Bay Area, China: Status quo and future scenarios. *Sci. Total Environ.* **2021**, *792*, 148427. [CrossRef] [PubMed]
2. Ji, J.; Li, P.; Chen, M.; Zhang, R.; Zhou, W.; You, Z. Review on the fatigue properties of recycled asphalt concrete containing construction and demolition wastes. *J. Clean. Prod.* **2021**, *327*, 129478. [CrossRef]
3. Yu, H.; Ma, T.; Wang, D.; Wang, Z.; Lv, S.; Zhu, X.; Liu, P.; Li, F.; Xiao, Y.; Zhang, J.; et al. Review on China's pavement engineering research 2020. *China J. Highw. Transp.* **2020**, *33*, 1–66.
4. Leite, F.d.C.; Motta, R.d.S.; Vasconcelos, K.L.; Bernucci, L. Laboratory evaluation of recycled construction and demolition waste for pavements. *Constr. Build. Mater.* **2011**, *25*, 2972–2979. [CrossRef]
5. Riviera, P.P.; Bassani, M.; Tefa, L.; Lillo, F. Use of cement kiln dust to stabilize construction and demolition waste for pavement applications. In Proceedings of the 95th TRB Annual Meeting, Washington, DC, USA, 10–14 January 2016.
6. Pasetto, M.; Baldo, N. Recycling of waste aggregate in cement bound mixtures for road pavement bases and sub-bases. *Constr. Build. Mater.* **2016**, *108*, 112–118. [CrossRef]
7. Xiao, J.; Chen, Q.; Wu, C.; Sun, Y.; Long, C. Fatigue performance of cement stabilized recycled brick and concrete aggregate (RBAC) mixtures. *J. Build. Mater.* **2019**, *22*, 922–927.
8. Zeng, M.; Tian, Z.; Xiao, J.; Wu, C. Performance of cement stabilized crushed stone pavement base materials containing construction waste. *J. Wuhan Univ. Technol.* **2016**, *38*, 34–38.
9. Zhang, J.H.; Li, C.; Ding, L.; Li, J. Performance evaluation of cement stabilized recycled mixture with recycled concrete aggregate and crushed brick. *Constr. Build. Mater.* **2021**, *296*, 123596. [CrossRef]
10. Disfani, M.M.; Arulrajah, A.; Haghighi, H.; Mohammadinia, A.; Horpibulsuk, S. Flexural beam fatigue strength evaluation of crushed brick as a supplementary material in cement stabilized recycled concrete aggregates. *Constr. Build. Mater.* **2014**, *68*, 667–676. [CrossRef]
11. Xuan, D.X.; Molenaar, A.A.A.; Houben, L.J.M. Evaluation of cement treatment of reclaimed construction and demolition waste as road bases. *J. Clean. Prod.* **2015**, *100*, 77–83. [CrossRef]
12. Xie, L.J. The Study on the Productive Technical and Properties of Recycled Brick Concrete. Master's Thesis, Shandong Agricultural University, Tai'an, China, 2012.
13. Park, D.Y.; Buch, N.; Chatti, K. Effective layer temperature prediction model and temperature correction via falling weight deflectometer deflections. *Transp. Res. Rec. J. Transp. Res. Board* **2001**, *1764*, 97–111. [CrossRef]
14. Chen, M. Study on Fatigue Performance of Recycled Aggregate Asphalt Mixture of Concrete Construction Waste Under Temperature Humidity Coupling. Master's Thesis, Beijing University of Civil Engineering and Architecture, Beijing, China, 2022.
15. *JTG/T F20-2015*; Technical Guidelines for Construction of Highway Roadbases. China Communications Press Co., Ltd.: Beijing, China, 2015.
16. Mohammadinia, A.; Arulrajah, A.; Sanjayan, J.; Disfani, M.M.; Bo, M.W.; Darmawan, S. Laboratory evaluation of the use of cement-treated construction and demolition materials in pavement base and subbase applications. *J. Mater. Civ. Eng.* **2015**, *27*, 04014186. [CrossRef]
17. Ji, X.P.; Cao, H.L.; Liu, L.Q. Performance and influencing factors of cement stabilized recycled concrete aggregate. *J. Build. Mater.* **2016**, *19*, 342–346.
18. Zhou, M.; Li, Z.; Wu, Y.; Zhang, X.; Ai, L. Experimental research on Lime-Fly Ash-Cement stabilized coal gangue mixture. *J. Build. Mater.* **2010**, *13*, 213–217.
19. *JTG D40-2011*; Code for Pavement Design of Urban Road. China Architecture & Building Press: Beijing, China, 2011.
20. Chen, K.; Suan, F.; Liang, S.; Zhang, H. Experimental study on frost resistance and crack resistance of bases in cold areas based on vibration mixing technology. *Mater. Rep.* **2021**, *35*, 291–296.
21. Wang, Y.Q.; Tan, Y.Q.; Guo, M.; Liu, Z.Y.; Wang, X.L. Study on the dynamic compressive resilient modulus and frost resistance of semi-rigid base materials. *Road Mater. Pavement Des.* **2017**, *18*, 259–269. [CrossRef]
22. *JTG D50-2017*; Specification for Design of Highway Asphalt Pavement. China Communications Press Co., Ltd.: Beijing, China, 2017.
23. Yue, G.B.; Li, Q.Y.; Luo, J.L.; Guo, Y.X. Influence of quality and replacement rate of recycled coarse aggregate on the frost resistance of recycled concrete. *Mater. Sci. Forum* **2017**, *898*, 2046–2049. [CrossRef]
24. Cui, R. Research on the Development of Structure and Material Performance of Semi-Rigid Base. Master's Thesis, Southeast University, Nanjing, China, 2019.
25. Sun, S. Study on the Modulus of Semi-Rigid Basic Structure of End-Serving Pavement. Master's Thesis, Chongqing Jiaotong University, Chongqing, China, 2014.
26. Zhang, J.Y. Semi-rigid base materials road performance. *Technol. Econ. Areas Commun.* **2012**, *14*, 74–75+78.
27. Li, X. Research on Value of Strength and Modulus of Cement-Stabilized Crushed Rock for Pavement Base Course. Master's Thesis, Chang'an University, Xi'an, China, 2016.

28. Lai, J. Researching on Mechanical Behaviors and Fatigue Properties of Cement Stabilized Recycled Aggregate Pavement Base. Master's Thesis, Fuzhou University, Fuzhou, China, 2017.
29. Liu, Z. Study on the Initial Durability of Semi-Rigid Base Material. Master's Thesis, Chongqing Jiaotong University, Chongqing, China, 2014.
30. Wang, C.; Lu, Y.; Zhang, Y.; Wu, H.; Ma, Z. Computed tomography images and digital volume correlation analysis of microstructural damage evolution in carbonated recycled aggregate concrete. *Constr. Build. Mater.* **2025**, *491*, 142761. [CrossRef]
31. Wei, J. Research on Fatigue Damage of Semi-Rigid Material and Structure of Asphalt Pavement. Ph.D. Thesis, Chang'an University, Xi'an, China, 2014.
32. *JTG E42-2005*; Test Methods for Aggregate for Highway Engineering. China Communications Press Co., Ltd.: Beijing, China, 2005.
33. *JTG/T 2321-2021*; Technical Specifications for Utilization of Construction Waste in Highway Engineering. China Communications Press Co., Ltd.: Beijing, China, 2021.
34. *JTG E30-2005*; Test Methods for Cement and Concrete for Highway Engineering. China Communications Press Co., Ltd.: Beijing, China, 2005.
35. *JTG E51-2009*; Test Methods of Materials Stabilized with Inorganic Binders for Highway Engineering. China Communications Press Co., Ltd.: Beijing, China, 2009.